Active vibration control based on piezoelectric smart composite

2013 Smart Mater. Struct. 22 125032

(http://iopscience.iop.org/0964-1726/22/12/125032)

Smart Mater. Struct. **22** (2013) 125032 (12pp) doi:10.1088/0964-1726/22/12/125032

Active vibration control based on piezoelectric smart composite

Le Gao[1], Qingqing Lu[1], Fan Fei[1], Liwu Liu[2], Yanju Liu[2] and Jinsong Leng[1]

[1] Centre for Composite Materials, Science Park of Harbin Institute of Technology (HIT), PO Box 3011, No. 2 YiKuang Street, Harbin 150080, People's Republic of China
[2] Department of Astronautical Science and Mechanics, Harbin Institute of Technology (HIT), PO Box 301, No. 92 West Dazhi Street, Harbin 150001, People's Republic of China

E-mail: lengjs@hit.edu.cn

Received 27 May 2013, in final form 20 October 2013
Published 22 November 2013
Online at stacks.iop.org/SMS/22/125032

Abstract
An aircraft's vertical fin may experience dramatic buffet loads in high angle of attack flight conditions, and these buffet loads would cause huge vibration and dynamic stress on the vertical fin structure. To reduce the dynamic vibration of the vertical fin structure, macro fiber composite (MFC) actuators were used in this paper. The drive moment equations and sensing voltage equations of the MFC actuators were developed. Finite element analysis models based on three kinds of models of simplified vertical fin structures with surface-bonded MFC actuators were established in ABAQUS. The equivalent damping ratio of the structure was employed in finite element analysis, in order to measure the effectiveness of vibration control. Further, an open-loop test for the active vibration control system of the vertical fin with MFC actuators was designed and developed. The experimental results validated the effectiveness of the MFC actuators as well as the developed methodology.

(Some figures may appear in colour only in the online journal)

1. Introduction

The vertical fin of an aircraft would experience a vibration problem due to an aeroelastic phenomenon called buffeting during fight conditions [1]. The buffeting occurs when the aircraft undergoes maneuvers involving high angles of attack. The intense and unsteady buffeting aerodynamic loads are characterized by a broadband spectrum with narrowband peak distributions. As a result, the lower vibration modes of the vertical tail are excited and introduce significant high-level dynamic stresses to the fin and empennage structures [2]. In order to find a solution for this technical problem, an active vibration control technology with real-time monitoring and prominent control capabilities is becoming more and more popular due to the increasingly stringent requirements of vibration reduction. If it features a network of actuators and sensors, computational capabilities and smart materials it will have a tremendous impact on conventional passive vibration control technology. Due to their broad bandwidth and quick response, piezoelectric materials are the most commonly used smart materials in active vibration control, and also can be employed as both actuators and sensors in the development of basic structures (e.g., beams, plates, shells) by taking advantage of direct and inverse piezoelectric effects.

The direct piezoelectric effect is widely used in sensors and energy harvesters, and the inverse piezoelectric effect in actuators such as ultrasonic welders and ultrasonic motors. Using piezoelectric film actuators, Choi and Sohn proposed a novel discrete-time sliding mode controller in order to alleviate undesirable chattering in vibration control of a flexible beam structure [3]. Maillard and Fuller gave analytical and experimental results of their investigation of active control of sound radiated from cylinders with piezoelectric actuators [4]. Raja *et al* designed a composite plate wing, surface bonded with eight piezoelectric bender actuators and sensors, and a modal flutter control model was formulated in state-space domain using coupled piezoelectric finite element procedures; the bending–torsion flutter instability was actively postponed using the energy imparted by the multilayered piezoelectric actuators [5]. Raja and Upadhya

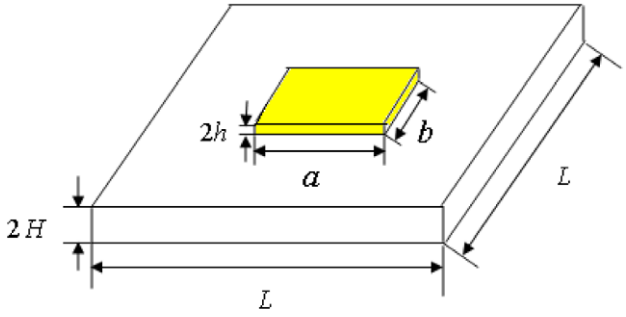

Figure 1. Plate model with macro fiber composite.

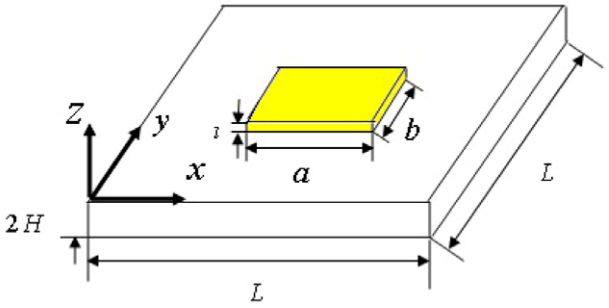

Figure 3. Reference coordinate axes of the plate model with MFC.

designed a wing model, and tested it in a 1.5 m low-speed wind tunnel; the experiment showed that the use of control surface aerodynamics was efficient in controlling the flutter characteristics of the vibrating aeroelastic system [6]. Karpel and Moulin established a model for aeroservoelastic analysis with smart structures, and a numerical application for an unmanned aerial vehicle with a piezoelectric-driven control surface was simulated [7]. Breitsamter conducted an experiment on active aerodynamic control for fin-buffeting alleviation; the considered eigen modes could be reduced by as much as 60% at angles of attack up to 31° [8].

Piezoelectric materials are the most popular amongst smart materials. Piezoelectric materials have received the most attention because of certain features such as low mass, low-cost, broad bandwidth, great bondability and embeddability within basic structures. In the mid-1990s, NASA successfully manufactured an excellent macro fiber composite (MFC) which integrates actuating and sensing abilities [9]. More and more researchers have been attracted to the investigation of the mechanical properties and industrial applications of MFC actuators or sensors. Park and Kim discussed the mechanical properties of single crystal MFC [10]. Paradies and Ciresa designed a wing for an unmanned aerial vehicle (UAV) with a thin profile and integrated roll control with piezoelectric elements [11]. Leng and Asundi designed an active vibration control system of smart structures based on a fiber optic sensor (FOS) and an electrorheological actuator [12]. Mudupu *et al* focused on the design and validation of a fuzzy logic controller for the smart fin of a projectile. The results showed that the proposed controller accomplished the desired fin angle control under various operating conditions [13]. Shin *et al* designed and manufactured an active twist rotor blade for vibration reduction in helicopters by using MFC actuators [14]. Schröck *et al* accomplished the control of a flexible beam actuated by macro fiber composite by simulation and experiments [15]. Henry *et al* discussed the applications of MFC for vibration suppression and structural health monitoring, and the experimental results showed the potential application of MFC for use in the dynamic control of flexible structures [16]. Yi conducted a vibration control experiment on a cantilever beam and a honeycomb aluminous panel [17]. Adetona *et al* discussed the employment of MFC for new inflatable/rigidizable hexapod structures; the experimental results showed its effectiveness in the dynamic control for effective application in dynamic control of inflatable structures [18]. Finite element analysis of the F-16 ventral fin was established by Robert *et al* [19]. Chen *et al* conducted a vibration control test of a full-scale F/A-18 ventral fin with multiple macro fiber composite actuators [20]. An adaptive controller of a smart fin was developed in [21]. This controller was based on the inverse feedback linearization technique. A special inspection was performed every 200 flight hours to monitor structural damage induced at the root of the F/A-18 vertical stabilizer [22]. Sohn *et al* discussed the optimal place for piezoelectric composite actuators to be applied for vibration control of a smart hull structure [23]. Kegong Wu investigated the piezoelectric actuating and sensing mechanism of a composite material structure with embedded piezoceramics [24]. Sohn *et al* completed the dynamic modeling of a smart hull structure with advanced MFC actuators. The control performance of the structure was also studied in order to suppress structural vibration of the system [25].

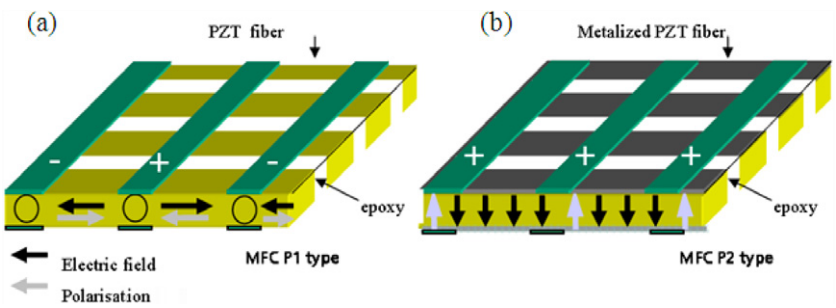

Figure 2. Explanation of the different types of MFC (P1 type and P2 type) [26].

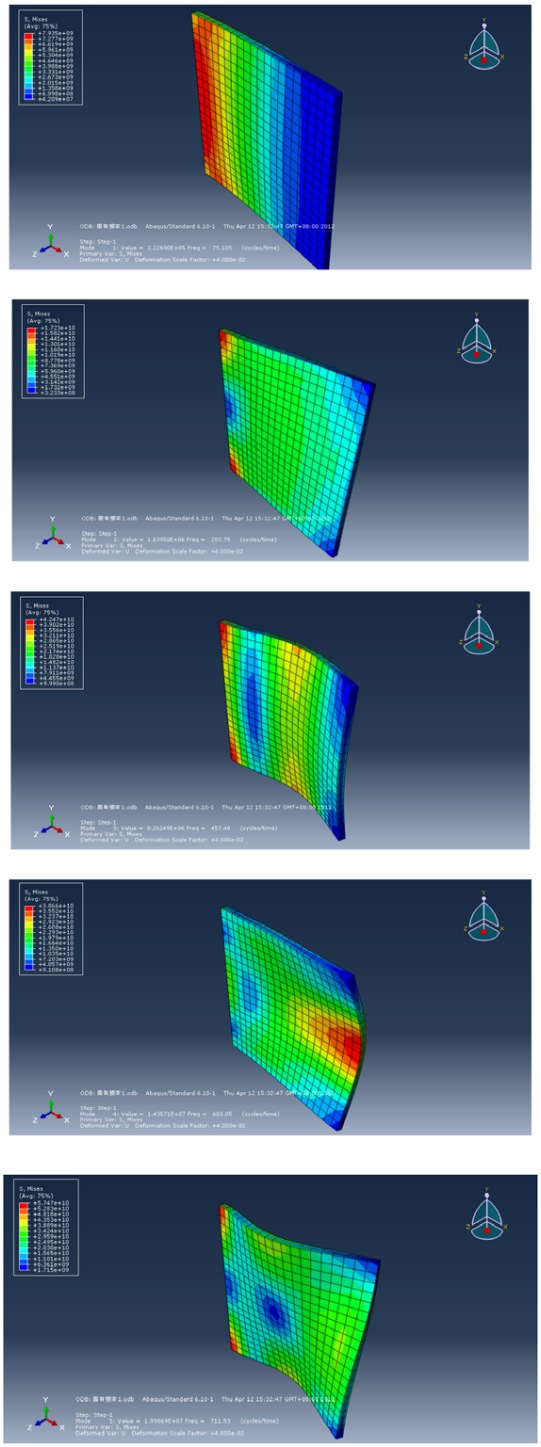

Figure 4. The first five modes of the cantilever plate without MFC.

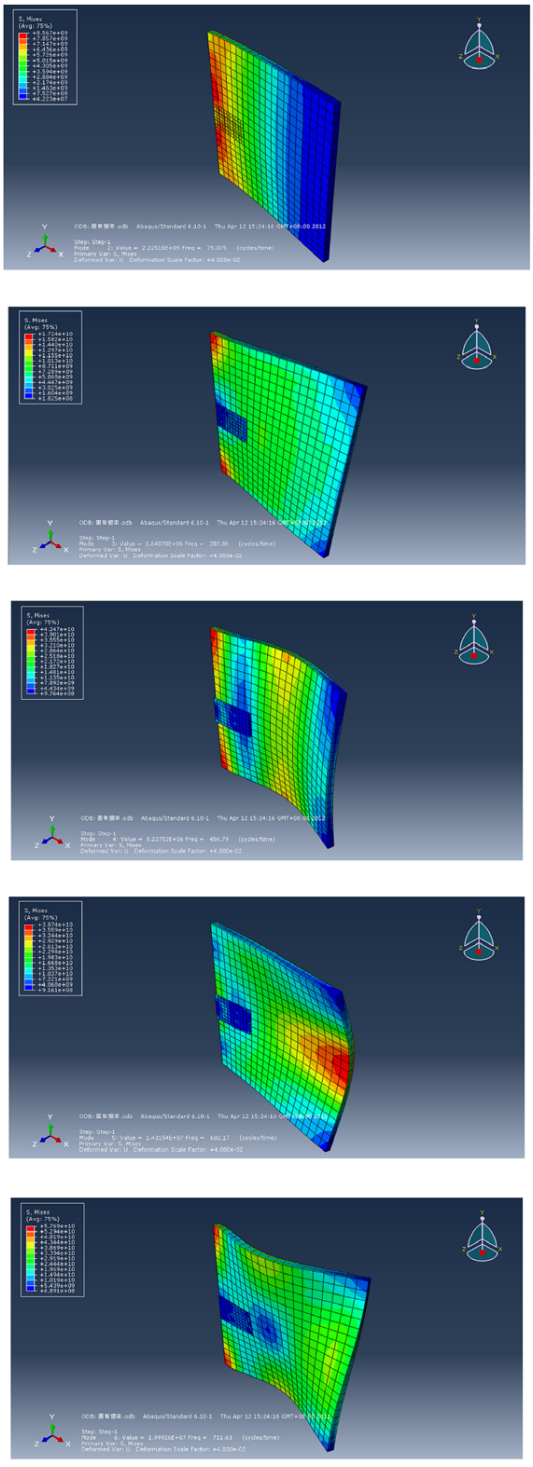

Figure 5. The first five modes of the cantilever plate with MFC.

The main work of this paper is to obtain the actuating equation when the MFC (d_{31} mode) works as an actuator, and the sensing equation when the MFC (d_{31} mode) works as a sensor. The finite element model of the vertical fin is established, and three simplified models are also introduced in order to accomplish the vibration control simulation. Further, an active vibration control open-loop test for the vertical fin model on which MFC is surface bonded is designed and developed.

2. The actuating and sensing equations of MFC

2.1. Piezoelectric constitutive equations

In this section, the two-dimensional piezoelectric constitutive equations of micro fiber composite are developed. On the one hand, macro fiber composite consisting of piezoelectric fibers and resin can perform distortion when subjected to external forces, which is the result of the special mechanical properties of piezoelectric materials. In the case of small

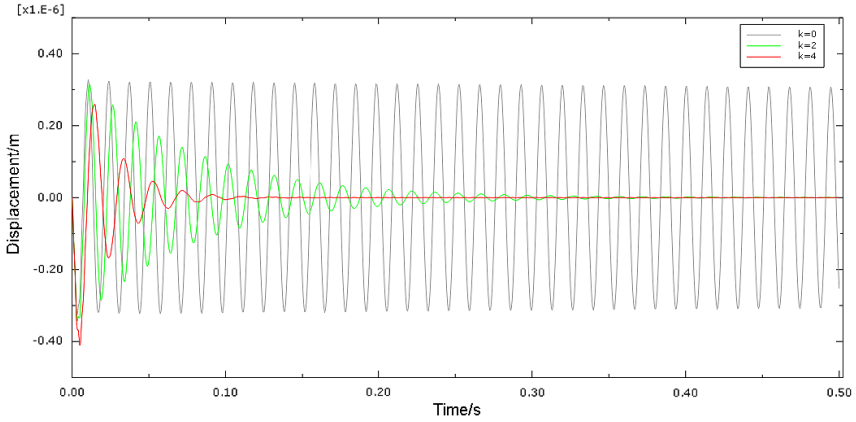

Figure 6. The free end displacement of the cantilever plate under control in the situation of undamped free vibration.

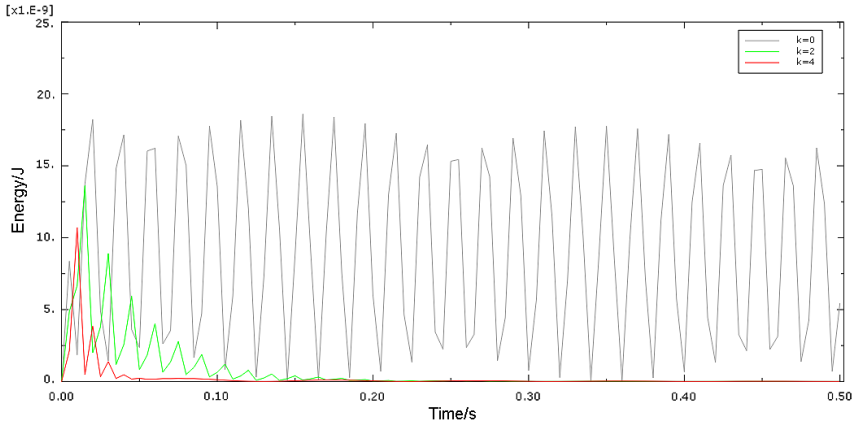

Figure 7. The kinetic energy curve at different values of K.

Table 1. The parameters of MFC used in finite element analysis.

Piezoelectric strain constant	$d_{31} = -1.7 \times 10^{-10}$ C N^{-1}		
Elastic constant	$E_1 = 15.857$ GPa	$E_2 = 15.857$ GPa	$E_3 = 30.336$ GPa
	$\mu_{12} = 0.31$	$\mu_{13} = 0.31$	$\mu_{23} = 0.31$
	$G_{31} = 5.515$ GPa	$G_{23} = 5.515$ GPa	$G_{12} = 6.052$ GPa
Permittivity	$\varepsilon_{33}^{\sigma} = 1.301 \times 10^{-8}$ F m^{-1}		
Density	$\rho_{\mathrm{MFC}} = 7750$ kg m^{-3}		

Table 2. The first five natural frequencies of the cantilever plate.

Natural frequency (Hz)	First mode	Second mode	Third mode	Fourth mode	Fifth mode
Without MFC	75.105	203.79	457.48	603.05	711.53
With MFC	75.075	203.86	456.79	602.17	711.63

deformation, MFC's stress–strain relationship follows the constitutive theory of elastic materials. On the other hand, due to the direct piezoelectric effect, positive and negative charges gather in its opposite surfaces and produce electric displacement. At the same time, under the influence of the electric field, the charge's movement generates electric strain and makes the material deform. Combining the mechanical and electrical properties, the linear constitutive relations for MFC can be expressed as follows:

$$\begin{bmatrix} \varepsilon \\ D \end{bmatrix} = \begin{bmatrix} s^E & d \\ d_t & \varepsilon^{\sigma} \end{bmatrix} \begin{bmatrix} \sigma \\ E \end{bmatrix} \tag{1}$$

where S^E represents all elements of the compliance matrix in a constant external electric field, d_t represents the piezoelectric

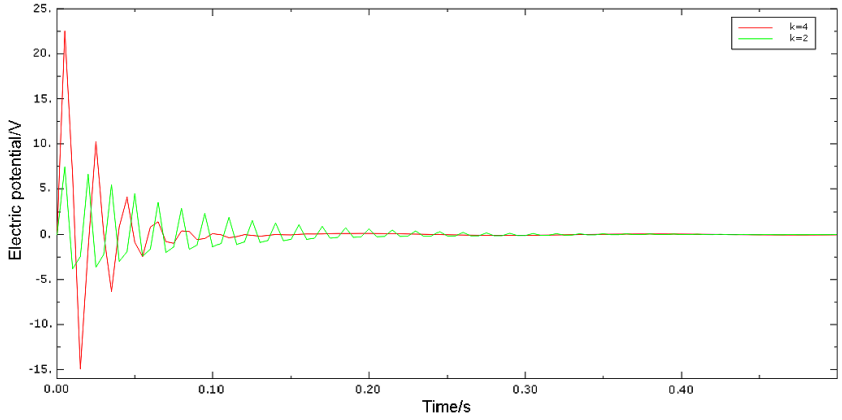

Figure 8. The feedback voltage–time curves under feedback control.

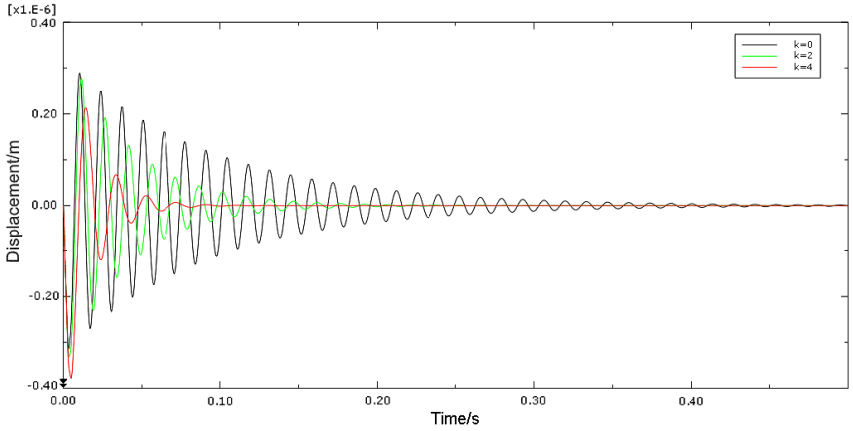

Figure 9. The free end displacement of the cantilever plate with $\xi = 0.0325$.

constants, and ε^{σ} refers to the dielectric constants in a static field.

It must be noted that MFC only has one layer of piezoelectric fiber sheet and its thickness is much smaller than its length and width, so MFC can be regarded as a simple laminate. Since the shear stress component does not affect the electric displacement and MFC can only be subjected to the electric field intensity in one direction, E_z, in actual working conditions, MFC's two-dimensional piezoelectric constitutive equations can be written as follows:

$$\begin{bmatrix} \varepsilon_x \\ \varepsilon_y \\ \varepsilon_z \\ D_z \end{bmatrix} = \begin{bmatrix} s_{11}^E & s_{12}^E & s_{13}^E \\ s_{12}^E & s_{11}^E & s_{13}^E \\ s_{13}^E & s_{13}^E & s_{33}^E \\ d_{31} & d_{31} & d_{33} \end{bmatrix} \begin{bmatrix} \sigma_x \\ \sigma_y \\ \sigma_z \end{bmatrix} + \begin{bmatrix} d_{31} \\ d_{31} \\ d_{33} \\ \varepsilon_{33}^{\sigma} \end{bmatrix} E_z. \quad (2)$$

2.2. The actuating equation of MFC

Macro fiber composite actuators can be surface bonded to a structure in high strain areas with or without minimal modification of the original structure or embedded into a structure such as in a plate model. Wu has studied the mechanical properties of a composite beam containing piezoelectric ceramic material, and summarized the mechanism of the piezoelectric composite structures with surface bonded MFC actuators [24]. The plate structure on which MFC is surface bonded is shown in figure 1.

MFC is available in d_{33} and d_{31} operational modes, a unique feature of macro fiber composite. Figure 2(a) shows the d_{33} effect, denoted by MFC P1 type; figure 2(b) shows the d_{31} effect, denoted by MFC P2 type [26]. Both MFC P1 and MFC P2 can be used as actuators and sensors, but MFC P2 type has a higher output force due to better stiffness. Therefore, in this work, MFC P2 has been used, which is produced by Smart Materials Corp.

From figure 2, the mechanical displacement of a d_{31} actuator is in the perpendicular direction to the applied electric voltage. The configuration and reference coordinate axes of MFC are presented in figure 3. As the stress component σ_z can be ignored, the two-dimensional form of equation (2) is easily obtained as follows:

$$\begin{bmatrix} \varepsilon_x \\ \varepsilon_y \end{bmatrix} = \begin{bmatrix} s_{11}^E & s_{12}^E \\ s_{12}^E & s_{11}^E \end{bmatrix} \begin{bmatrix} \sigma_x \\ \sigma_y \end{bmatrix} + \begin{bmatrix} d_{31} \\ d_{31} \end{bmatrix} E_z. \quad (3)$$

Subsequently, with the MFC exposed in a certain electric field, the moment equation of MFC actuators can be

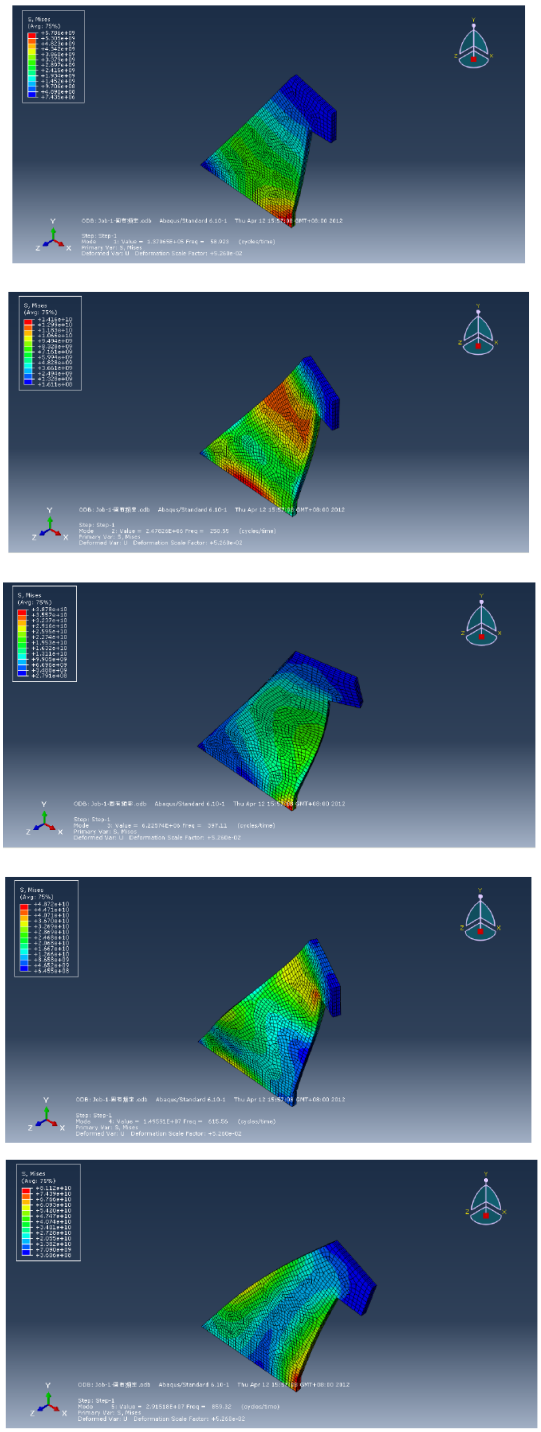

Figure 10. The first five modes of the planar model of a vertical fin structure.

written as

$$M_x = b\int_H^{H+2h}(-\sigma_x)z\,\mathrm{d}z = b\int_H^{H+2h}\left[Q_{11}^E(d_{31}E_z-\varepsilon_x) + Q_{12}^E(d_{31}E_z-\varepsilon_y)\right]z\,\mathrm{d}z$$
$$M_y = a\int_H^{H+2h}(-\sigma_y)z\,\mathrm{d}z = a\int_H^{H+2h}\left[Q_{12}^E(d_{31}E_z-\varepsilon_x) + Q_{11}^E(d_{31}E_z-\varepsilon_y)\right]z\,\mathrm{d}z \quad (4)$$

where L is the length and width of the plate and $2H$ is the thickness; for the MFC, the length is a, the width is b, and the thickness is $2h$. Assuming that the bonding between the MFC and the plate structure is perfect, due to the relationship $h \ll H$, we can stipulate the approximations that $H+h \to H$ and $H+2h \to H$. Through substitution of the neutral layer's curvature formula, $\varepsilon_x = \frac{z}{\rho_x}$, $\varepsilon_y = \frac{z}{\rho_y}$ and $\rho = \frac{E_z I}{M(1-\mu_z)}$, and the electric field intensity equation, $E_z = \frac{U}{2h}$, equation (4) becomes

$$M_x = \frac{(b+AabQ_{11}^E - AabQ_{12}^E)(Q_{11}^E+Q_{12}^E)}{(1+AaQ_{11}^E)(1+AbQ_{11}^E)-A^2ab(Q_{12}^E)^2}d_{31}UH$$
$$M_y = \frac{(a+AabQ_{11}^E - AabQ_{12}^E)(Q_{11}^E+Q_{12}^E)}{(1+AaQ_{11}^E)(1+AbQ_{11}^E)-A^2ab(Q_{12}^E)^2}d_{31}UH \quad (5)$$

where

$$Q_{11}^E = \frac{s_{11}^E}{(s_{11}^E)^2-(s_{12}^E)^2}, \qquad Q_{12}^E = \frac{-s_{12}^E}{(s_{11}^E)^2-(s_{12}^E)^2}. \quad (6)$$

2.3. The sensing equation of MFC

Due to the piezoelectric effect, when MFC obtains a deformation, the charge will move, and an electric displacement is formed. As the stress component σ_z can be ignored, we can obtain

$$D_z = d_{31}(\sigma_x+\sigma_y)+\varepsilon_{33}^{\sigma}E_z = \frac{d_{31}(Q_{11}^E+Q_{12}^E)(\varepsilon_x+\varepsilon_y)}{1+[2d_{31}^2(Q_{11}^E+Q_{12}^E)-\varepsilon_{33}^{\sigma}]\cdot\frac{A_{\mathrm{MFC}}}{C_{\mathrm{MFC}}\cdot 2t}} \quad (7)$$

$$E_z = \frac{d_{31}(Q_{11}^E+Q_{12}^E)(\varepsilon_x+\varepsilon_y)}{\frac{C_{\mathrm{MFC}}\cdot 2t}{A_{\mathrm{MFC}}}+2d_{31}^2(Q_{11}^E+Q_{12}^E)-\varepsilon_{33}^{\sigma}}. \quad (8)$$

Note that $t = h$, so the sensing equation is obtained,

$$U_{\mathrm{out}} = E_z\cdot 2t = \frac{2td_{31}(Q_{11}^E+Q_{12}^E)(\varepsilon_x+\varepsilon_y)}{\frac{C_{\mathrm{MFC}}\cdot 2t}{A_{\mathrm{MFC}}}+2d_{31}^2(Q_{11}^E+Q_{12}^E)-\varepsilon_{33}^{\sigma}} = \frac{2hd_{31}(Q_{11}^E+Q_{12}^E)(\varepsilon_x+\varepsilon_y)}{\frac{C_{\mathrm{MFC}}\cdot 2h}{A_{\mathrm{MFC}}}+2d_{31}^2(Q_{11}^E+Q_{12}^E)-\varepsilon_{33}^{\sigma}} = K\cdot(\varepsilon_x+\varepsilon_y) \quad (9)$$

where K is defined as the feedback control factor.

3. Finite element analysis of basic structures using MFC

In this section, three kinds of simplified model for a vertical fin were established, including a cantilever plate structure, a planar model of a vertical fin structure, and an entity model of a vertical fin structure. The material in these models is aluminum; the elastic modulus is 68 GPa and the Poisson ratio is 0.32. The parameters of MFC which we used in the finite element analysis are shown in table 1.

According to the negative feedback control algorithm, the feedback voltage can be expressed as follows:

$$U_{\mathrm{in}} = -kU_{\mathrm{out}} \quad (10)$$

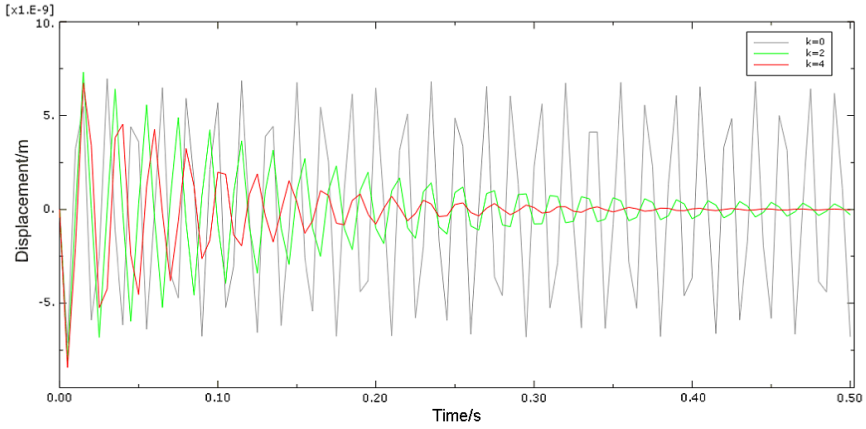

Figure 11. The free end displacement of the planar model of a vertical fin structure.

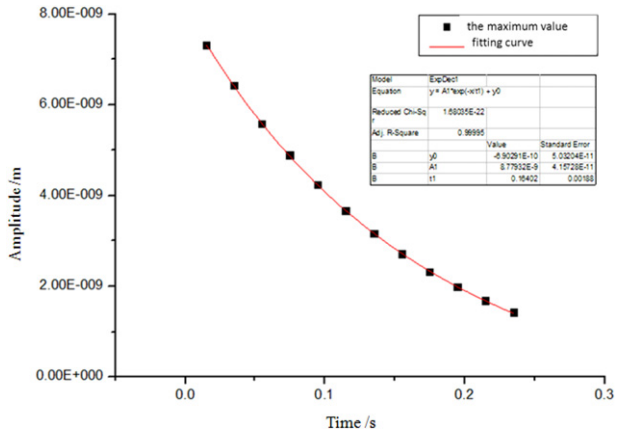

Figure 12. The fitting curve when $K = 2$.

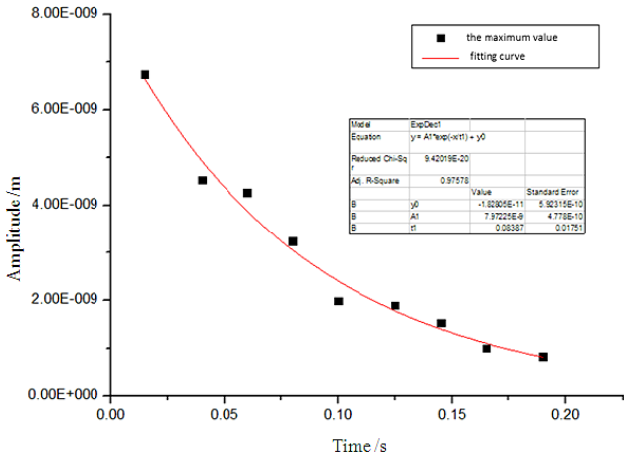

Figure 13. The fitting curve when $K = 4$.

where U_{in} is the control input, U_{out} is the sensor output, k is the feedback magnification factor, and its value is limited by the model's breakdown voltage.

From equation (9), we can obtain

$$U_{\text{in}} = -k \cdot K \cdot (\varepsilon_x + \varepsilon_y) = -k \cdot K \cdot \frac{u2 - u1}{\mathrm{d}x}. \qquad (11)$$

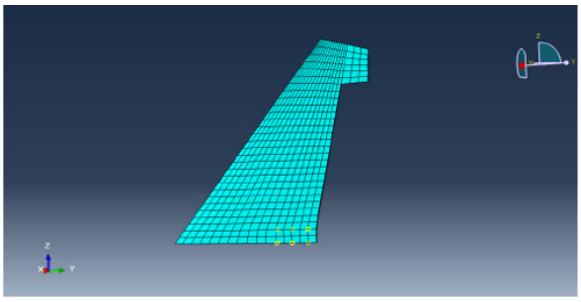

Figure 14. The finite element analysis model of the entity model.

Equation (11) is the mathematical formula that the ABAQUS subprogram UAMP depends on.

3.1. Active vibration control simulation for a cantilever plate structure

Active vibration control of the cantilever plate structure is simulated in this section. Figures 4 and 5 show a comparison between the first five modes for the cantilever plate with MFC and the one without MFC. From table 2, it can be seen that the MFC has little influence on the structure's resonance frequency.

Figure 6 shows the free end displacement of the cantilever plate under control in the case of undamped free vibration. When $K = 2$, the free end displacement reduces to zero after 10 periods. As K increases, the number of periods it needs to reach zero decreases. After three periods of control, with $K = 2$, the amplitude reduces to 67% of its original value. When $K = 4$, however, the amplitude reduces to 15%.

Therefore, as K increases, the attenuation of the free end displacement becomes faster and faster, and the frequency of the free end displacement decreases.

However, the vibration of the whole plate with a different feedback control factor cannot be analyzed by free end displacement, so the kinetic energy was taken into consideration. Figure 7 shows the kinetic energy curves at different values of K. When $K = 0$, the cantilever plate makes an undamped free vibration, and the kinetic energy follows

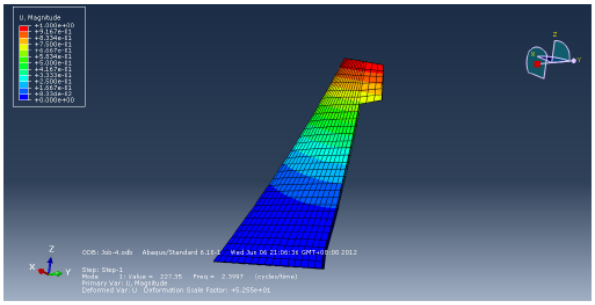

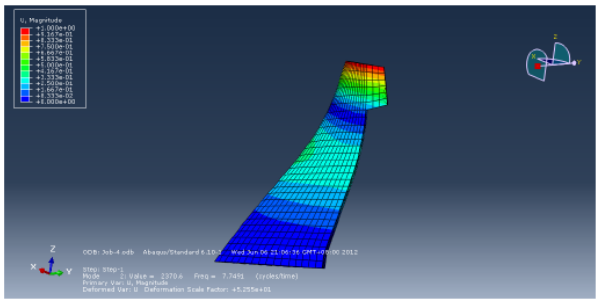

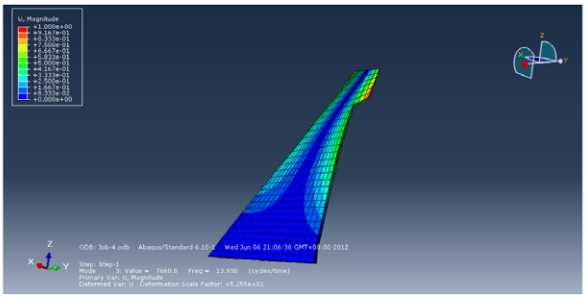

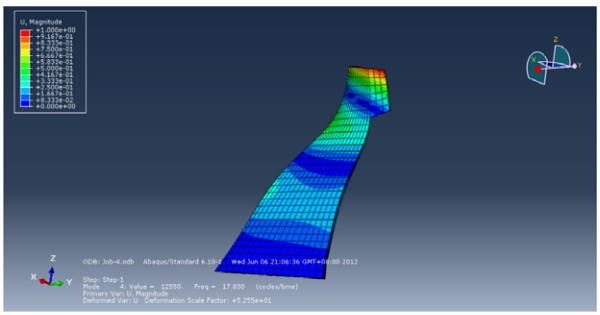

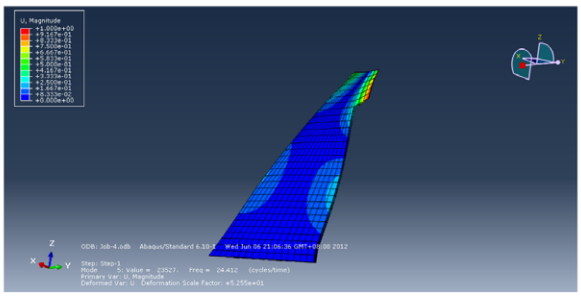

Figure 15. The first five modes of the entity model.

the periodical change rule. It is not difficult to conclude that the kinetic energy decreases rapidly under control.

Figure 8 shows the feedback voltage–time curves under feedback control. When $K = 0$, the time for complete

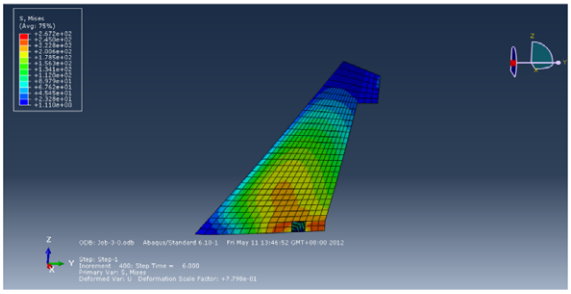

Figure 16. The strain field when a uniform load is applied to the model surface.

reduction of the displacement is 0.35 s; when K increases to 2, the time needed becomes 0.2 s; for $K = 4$, it is only 0.08 s. Therefore, the drive voltage of the MFC submits the periodical attenuation trend, and the larger K is, the faster it decays.

For other cases, taking the damping ratio of the cantilever plate equal to 0.0325, the results are shown in figure 9. Rayleigh's proportional damping is used in the analysis of the cantilever plate structure. With increase of K, the free end displacement decays exponentially faster. Therefore, the function of MFC actuators can be regarded as an additional damping ratio for the structure.

3.2. Active vibration control simulation for the planar model of a vertical fin structure

In this section, a planar model of a vertical fin structure is developed for the finite element analysis. Figure 10 shows the first five modes of the two-dimensional vertical fin model. The MFC should be located in the large vibration region with low order modes.

Figure 11 shows the free end displacement of the planar model of a vertical fin structure. Comparing with figure 9, we can use an equivalent damping ratio ξ to signify the function of the MFC actuators.

In the case of small damping ratio, the attenuation formula is as follows:

$$y = A\mathrm{e}^{-\xi\omega t} \tag{12}$$

where ξ is the damping ratio and ω is the natural frequency.

Further, to match the maximum value of the free end displacement when $K = 2$ and $K = 4$, the fitting formula can be written as follows:

$$y = A_1\mathrm{e}^{-\frac{x}{t_1}} + y_0. \tag{13}$$

Then the damping ratio ξ is as follows:

$$\xi = \frac{1}{\omega t_1} = \frac{1}{\frac{2\pi}{T}t_1} = \frac{T}{2\pi t_1}. \tag{14}$$

Therefore, the fitting curves when $K = 2$ and $K = 4$ are as shown in figures 12 and 13. Using the fitting coefficient t_1 in equation (14), the damping ratio ξ can be calculated. When $K = 2$, the damping ratio $\xi = 0.0194$, when $K = 4$, the damping ratio $\xi = 0.0415$. Based on the above analysis, the larger the feedback control factor is, the larger damping ratio we have.

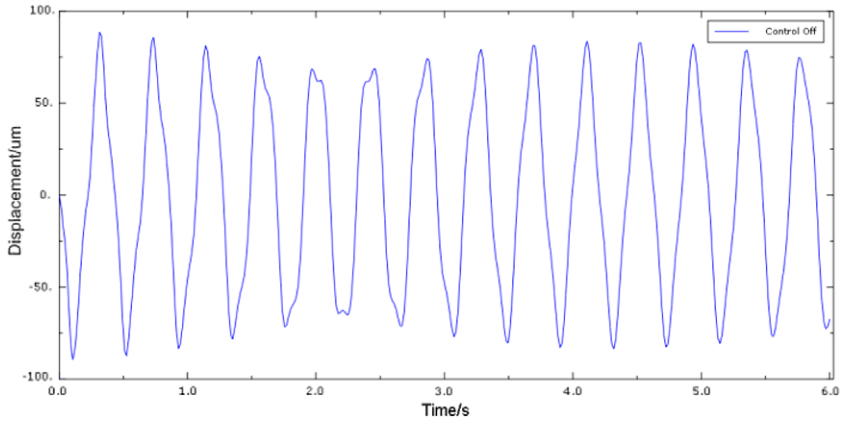

Figure 17. The free end displacement when a sinusoidal pressure is applied to the structure.

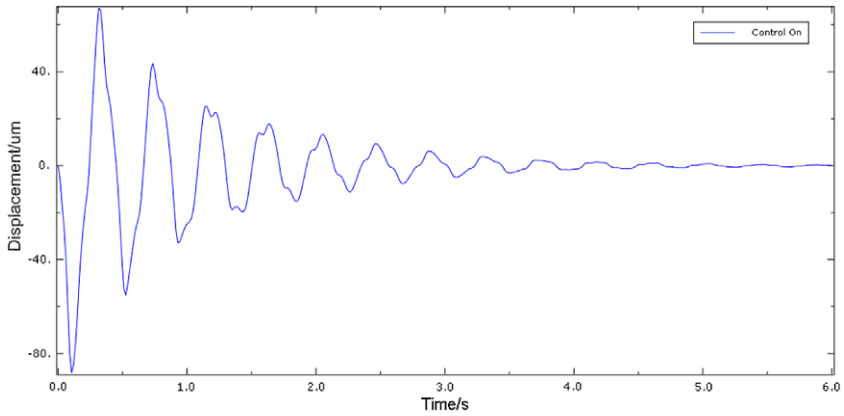

Figure 18. The free end displacement when voltage (300 V, 400 Hz) is applied to the MFC.

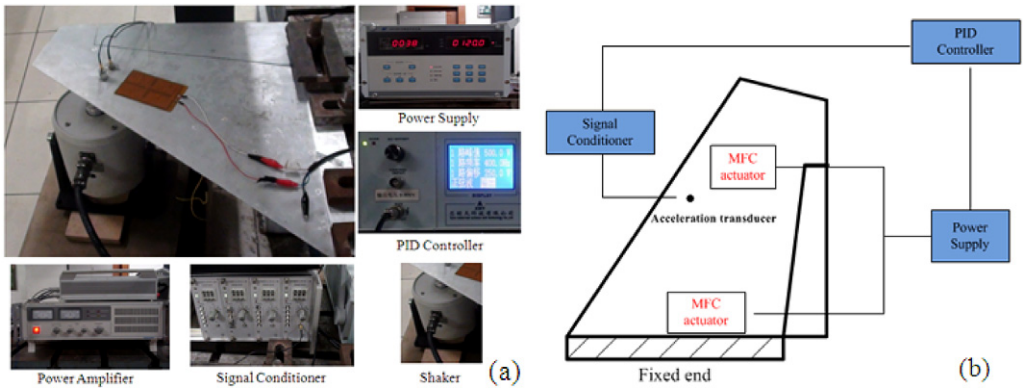

Figure 19. The experimental system of vertical fin vibration control.

3.3. Active vibration control simulation for the entity model of a vertical fin structure

In this section, the entity model of a vertical fin structure is developed for finite element analysis. Figure 14 shows the finite element analysis of the entity model of a vertical fin structure by ABAQUS. Figure 15 shows the first five modes of the entity model. When a uniform load is applied on the model surface, the maximum strain fields occur in the fixed part, as shown in figure 16. The purpose of vibration control is to restrain the strain fields. Under the condition of no voltage application, figure 17 illustrates the simulated response of the free end displacement when a sinusoidal pressure is implemented. An applied voltage (300 V, 400 Hz) on the MFC changes the free end displacement as in figure 18. Compared with figure 17, the amplitude of the free end displacement is reduced by 41% during one period, and after 10 periods, the displacement approaches 0. By exponential decay fitting, the

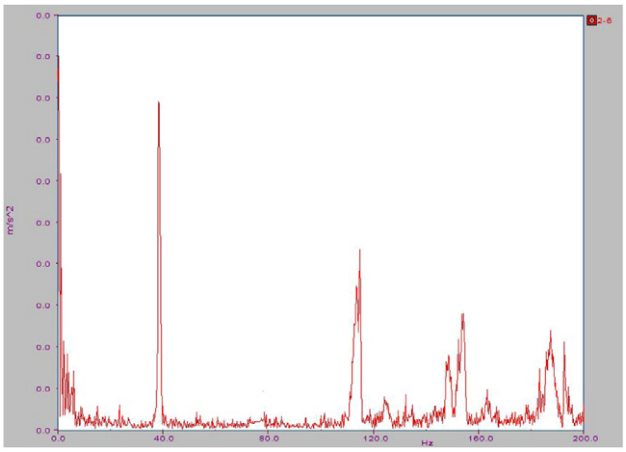

Figure 20. The first and second natural frequencies.

amplitude of the free end displacement decays according to the equivalent damping ratio $\xi = 0.007\,96$.

4. Experiments on active vibration control using MFC actuators

In this section, an active vibration control open-loop test of a vertical fin model is conducted. The experimental setup with vertical fin and MFC is shown in figure 19. The MFC analyzed in this experiment is manufactured by Smart Materials Corp. The MFC's operational voltage ranges from −500 to 1500 V. An open-loop test was designed to verify the validity of MFC actuators. In this experimental study,

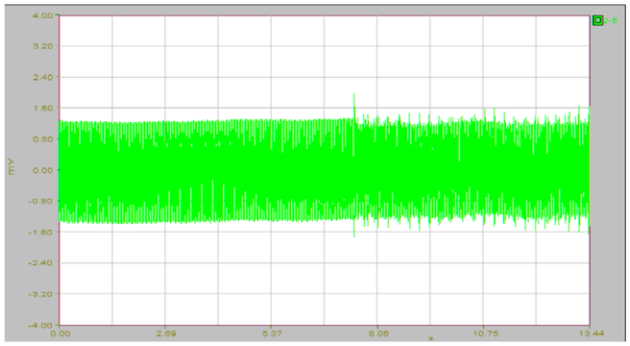

Figure 21. Vibration response when the excited frequency is equal to 40 Hz and the control voltage is equal to 400 V, 400 Hz.

MFC actuators are bonded to the surface of a vertical fin. An electromagnetic shaker is used to supply the original vibration of the vertical fin and the structural response is detected by an acceleration transducer. A multichannel PID controller is used in the vibration control experiment, which provides the analog control input to the MFC actuators.

Firstly, we experimentally measure the frequency response of the structure, as shown in figure 20. The first and second natural frequencies of the model are 38.8 and 115.2 Hz. In general, vibration reduction is mainly considered in the resonance region, so the excited frequencies can be selected as 40 and 120 Hz. With the steady state vibration at 40 and 120 Hz, the control voltage and frequency are selected to evaluate the performance of the closed-loop response.

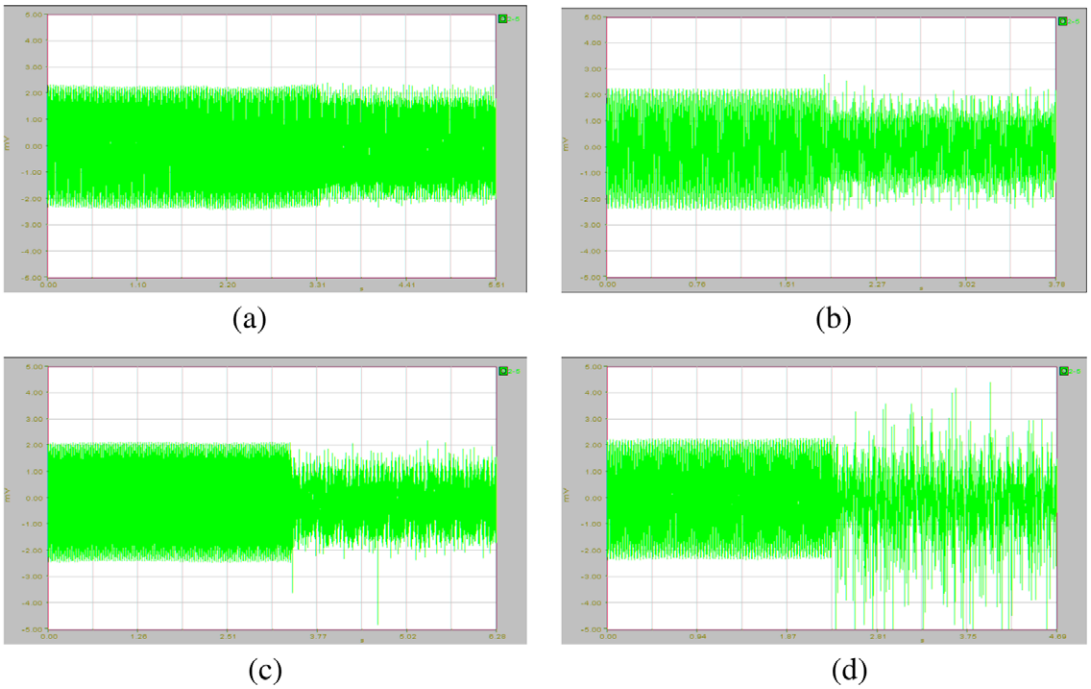

Figure 22. Vibration responses of different control voltages when the excited frequency is equal to 120 Hz and (a) the control voltage is equal to 450 V, 400 Hz, (b) the control voltage is equal to 450 V, 500 Hz, (c) the control voltage is equal to 450 V, 530 Hz, and (d) the control voltage is equal to 450 V, 550 Hz.

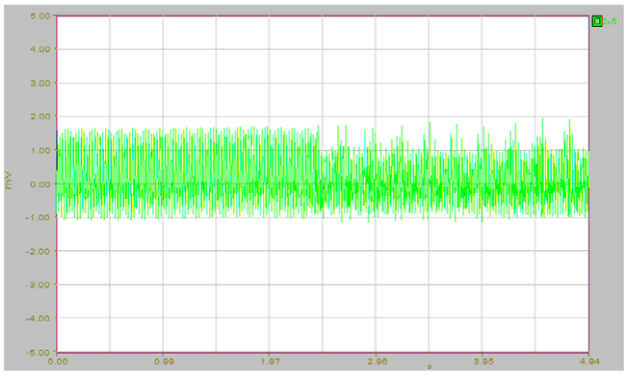

Figure 23. Vibration response when the excited frequency is equal to 40 Hz and the control voltage is equal to 310 V, 400 Hz.

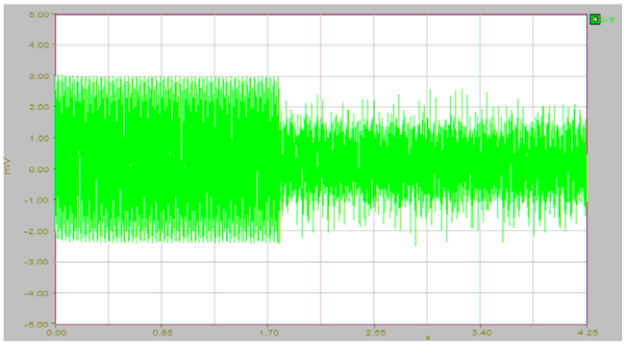

Figure 24. Vibration response when the excited frequency is equal to 120 Hz and the control voltage is equal to 310 V, 420 Hz.

4.1. Active vibration control for MFC actuators attached to the root region

In order to obtain an obvious result of the active vibration control experiment, we select the larger vibration region as the actuator location. As in figure 17, an MFC actuator is surface mounted to the root region. The decrease of vibration amplitude is investigated when a suitable control voltage and frequency are applied to the MFC actuator.

In this experiment, the structure is subjected to vibration with the help of an electromagnetic shaker. The controller voltage and frequency are then adjusted and the developed controlled signals are supplied to the MFC actuator. Accordingly the responses of the vertical fin are collected through an accelerometer to evaluate the closed-loop system performance.

When the excited frequency is 40 Hz, the damping effect is not very effective. Only when the control voltage is 400 V/400 Hz is the vibration suppressed by 5%, as shown in figure 21.

When the excited frequency is 120 Hz, the vibration of the controlled vertical fin is suppressed effectively by 30% more than it is in the corresponding uncontrolled case.

Figure 22 shows the vibration response at different control voltages. When the control voltage is 450 V/400 Hz, the vertical fin vibration is reduced by approximately 10%; when the voltage is adjusted to 450 V/530 Hz, the vibration is suppressed effectively by 30%. It can be easily concluded that in order to achieve a better reduction performance the control frequency should be in a certain range.

4.2. Active vibration control for MFC actuators attached to the middle region

In this section, the MFC actuator is pasted to the middle region of the vertical fin model. When the excited frequency is 40 Hz, by adjusting the control voltage and frequency of the MFC, the damping effect is not very obvious. Only when the control voltage is 310 V/400 Hz is the vibration suppressed by 10%, as shown in figure 23.

However, in the case where the excited frequency is 120 Hz, the vibration of the controlled vertical fin is suppressed effectively by more than 45% compared to the uncontrolled case. Figure 24 clearly shows the vibration response with the control voltage 310 V/420 Hz.

5. Conclusions

Piezoelectric materials are the most popular amongst smart materials. Macro fiber composite has the advantages of being lightweight, low-cost, surface bonded and easy-to-implement, and offers sensing and actuation capabilities that can be utilized for active vibration control. In this paper, the piezoelectric actuating and sensing equations were presented, three simplified models of a vertical fin with MFC actuators were proposed and their vibration control performance was evaluated. Based on the actuating equations and sensing equation, the piezoelectric feedback control factor was derived for the vibration control simulation. The active vibration control performance of the proposed systems was evaluated through experimental investigation. The results demonstrate that structural vibration can be effectively suppressed by using MFC actuators.

Acknowledgment

This work is supported by the National Natural Science Foundation of China (Grant Nos 1122521, 11272106).

References

[1] Hauch R M, Jacobs J H, Dima C and Ravindra K 1996 Reduction of vertical fin buffet response using active control *J. Aircr.* **33** 617–22

[2] Chen Y, Ulker F D, Nalbantoglu V, Wickramasinghe V, Zimcik D and Yaman Y 2009 Active control of smart fin model for aircraft buffeting load alleviation applications *J. Aircr.* **46** 1965–72

[3] Choi S B and Sohn J W 2006 Chattering alleviation in vibration control of smart beam structures using piezofilm actuators: experimental verification *J. Sound Vib.* **294** 640–9

[4] Maillard J P and Fuller C R 1999 Active control of sound radiation from cylinders with piezoelectric actuators and structural acoustic sensing *J. Sound Vib.* **222** 363–88

[5] Raja S, Pashilkar A A and Sreedeep R 2006 Flutter control of a composite plate with piezoelectric multilayered actuators *Aerosp. Sci. Technol.* **10** 435–41

[6] Raja S and Upadhya A R 2007 Active control of wing flutter using piezoactuated surface *J. Aircr.* **44** 71–80
[7] Karpel M and Moulin B 2004 Models for aeroservoelastic analysis with smart structures *J. Aircr.* **41** 314–21
[8] Breitsamter C 2005 Aerodynamic active control for fin-buffet load alleviation *J. Aircr.* **42** 1252–63
[9] Wilkie W K, Bryant R G, High J W, Fox R L, Hellbaum R F and Jalink A 2000 Low-cost piezocomposite actuator for structural control applications *Proc. SPIE* **3991** 323–34
[10] Park J S and Kim J H 2005 Analytical development of single crystal macro fiber composite actuators for active twist rotor blades *Smart Mater. Struct.* **14** 745–53
[11] Paradies R and Ciresa P 2009 Active wing design with integrated flight control using piezoelectric macro fiber composites *Smart Mater. Struct.* **18** 035010
[12] Leng J and Asundi A 1999 Active vibration control system of smart structures based on FOS and ER actuator *Smart Mater. Struct.* **8** 252–6
[13] Mudupu V, Trabia M B, Yim W and Weinacht P 2008 Design and validation of a fuzzy logic controller for a smart projectile fin with a piezoelectric macro-fiber composite bimorph actuator *Smart Mater. Struct.* **17** 035034
[14] Shin S-J 2001 Integral twist actuation of helicopter rotor blades for vibration reduction *PhD Dissertation* Department of Aeronautics and Astronautics, Massachusetts Institute of Technology
[15] Schröck J, Meurer T and Kugi A 2011 Control of a flexible beam actuated by macro-fiber composite patches: I. Modeling and feedforward trajectory control *Smart Mater. Struct.* **20** 015016
[16] Henry A S, Gyuhae P and Daniel J I 2004 An investigation into the performance of macro-fiber composites for sensing and structural vibration applications *Mech. Syst. Signal Process.* **18** 683–97
[17] Yi G, Liu Y J and Leng J S 2011 Active vibration control of basic structures using macro fiber composites *Proc. SPIE* **7977** 79772C
[18] Adetona O, Keel L H, Horta L G, Cadogan D P, Sapna G H and Scarborough S E 2002 Description of new inflatable/rigidizable hexapod structure testbed for shape and vibration control *AIAA/ASME/ASCE/AMS/ASC/ Structural Dynamics and Materials Conf.* vol 3, pp 2027–31
[19] Robert A C, Shawn D M and Donald L K 2008 Alleviation of buffet-induced vibration using piezoelectric actuators *Comput. Struct.* **86** 281–91
[20] Chen Y, Viresh W and Zimcik D 2006 Development and verification of real-time controllers for F/A-18 vertical fin buffet load alleviation *Proc. SPIE* **6173** 1–12
[21] Mani S, Singh S, Parimi S, Yim W and Trabia M 2005 Adaptive control of a projectile fin using piezoelectric elastic beam *AIAA Guidance, Navigation and Control Conf. and Exhibit* vol 3, pp 2247–57
[22] Moses R W 1997 Active vertical fin buffeting alleviation on a twin fin fighter configuration in a wind tunnel *CEAS Int. Forum on Aeroelasticity and Structural Dynamics (Rome, Italy, June)*
[23] Sohn J W, Choi S B and Kim H S 2011 Vibration control of smart hull structure with optimally placed piezoelectric composite actuators *Int. J. Mech. Sci.* **53** 647–59
[24] Wu K 2003 Theoretical and experimental study of active vibration control of intelligent composite material structures with embedded piezoceramics *PhD Thesis* Northwestern Polytechnical University Papers: 29-4
[25] Sohn J W, Kim H S, Kim C J, Hoon Ha S and Choi S B 2007 Vibration suppression of hull structure using macro fiber composite actuators and sensors *Proc. SPIE* **6525** 652527
[26] Schönecker1a A J, Daueb T, Brücknera B, Freytaga C, Hähnea L and Rödiga T 2006 Overview on macro fiber composite applications *Proc. SPIE* **6170** 61701K